



**HAL**  
open science

## Extracellular traps formation following cervical spinal cord injury

Pauline Michel-Flutot, Camille H. Bourcier, Laila Emam, Adeline Gasser,  
Simon Glatigny, Stéphane Vinit, Arnaud Mansart

► **To cite this version:**

Pauline Michel-Flutot, Camille H. Bourcier, Laila Emam, Adeline Gasser, Simon Glatigny, et al.. Extracellular traps formation following cervical spinal cord injury. *European Journal of Neuroscience*, 2023, 57 (4), pp.692-704. 10.1111/ejn.15902 . hal-04122495

**HAL Id: hal-04122495**

**<https://hal.science/hal-04122495>**

Submitted on 27 Jun 2023



**HAL** is a multi-disciplinary open access archive for the deposit and dissemination of scientific research documents, whether they are published or not. The documents may come from teaching and research institutions in France or abroad, or from public or private research centers.

L'archive ouverte pluridisciplinaire **HAL**, est destinée au dépôt et à la diffusion de documents scientifiques de niveau recherche, publiés ou non, émanant des établissements d'enseignement et de recherche français ou étrangers, des laboratoires publics ou privés.



Distributed under a Creative Commons Attribution - NonCommercial - NoDerivatives 4.0 International License

# Extracellular traps formation following cervical spinal cord injury

Pauline Michel-Flutot<sup>1</sup>  | Camille H. Bourcier<sup>1,2</sup> | Laila Emam<sup>2</sup> |  
Adeline Gasser<sup>2</sup> | Simon Glatigny<sup>2</sup> | Stéphane Vinit<sup>1</sup>  | Arnaud Mansart<sup>2</sup>

<sup>1</sup>Université Paris-Saclay, UVSQ, Inserm U1179, END-ICAP, Versailles, France

<sup>2</sup>Université Paris-Saclay, UVSQ, Inserm U1173, Infection et Inflammation (2I), France

## Correspondence

Pauline Michel-Flutot, Université Paris-Saclay, UVSQ, Inserm U1179, END-ICAP, Versailles 78000, France.

Email: [pauline.michel78280@yahoo.fr](mailto:pauline.michel78280@yahoo.fr)

## Funding information

Institut National de la Santé et de la Recherche Médicale; Chancellerie des Universités de Paris, Grant/Award Number: Legs Poix; INSERM; Université de Versailles Saint-Quentin-en-Yvelines; Fondation pour la recherche médicale, Grant/Award Number: ECO202106013756

Edited by: Francisco Alvarez

## Abstract

Spinal cord injuries involve a primary injury that can lead to permanent loss of function and a secondary injury associated with pathologic and inflammatory processes. Extracellular traps are extracellular structures expressed by immune cells that are primarily composed of chromatin, granular enzymes and histones. Extracellular traps are known to induce tissue damage when overexpressed and could be associated in the occurrence of secondary damage. In the present study, we used flow cytometry to demonstrate that at 1 day following a C2 spinal cord lateral hemisection in male Swiss mice, resident microglia form vital microglia extracellular traps, and infiltrating neutrophils form vital neutrophil extracellular traps. We also used immunolabelling to show that microglia near the lesion area are most likely to form these microglia extracellular traps. As expected, infiltrating neutrophils are located at the site of injury, though only some of them engage in post-injury extracellular trap formation. We also observed the formation of microglia and neutrophil extracellular traps in our sham animal models of durotomy, but formation was less frequent than following the C2 hemisection. Our results demonstrate for the first time that microglia form extracellular traps in the spinal cord following injury and durotomy. It remains however to determine the exact mechanisms and kinetics of neutrophil and microglia extracellular traps formation following spinal cord injury. This information would allow to better mitigate this inflammatory process that may contribute to secondary injury and to effectively target extracellular traps to improve functional outcomes following spinal cord injury.

**Abbreviations:** C2, second cervical; DAPI, 4',6-diamidino-2-phenylindole; dnase1, deoxyribonuclease-1; EDTA, ethylenediaminetetraacetic acid; ETs, extracellular traps; FMO, fluorescence minus one; h3cit, citrullinated histone H3; MDMs, monocyte-derived macrophages; METs, macrophage ETs; MFI, mean fluorescence intensity; MiETs, microglia ETs; MPO, myeloperoxidase; NDS, normal donkey serum; NETs, neutrophil extracellular traps; P.I., post-injury; PAD4, peptidylarginine deiminase 4; PBS, phosphate-buffered saline; ROS, reactive oxygen species; RPMI, Roswell Park Memorial Institute RT, room temperature.

Stéphane Vinit and Arnaud Mansart contributed equally to this work.

This is an open access article under the terms of the [Creative Commons Attribution-NonCommercial-NoDerivs](https://creativecommons.org/licenses/by-nc-nd/4.0/) License, which permits use and distribution in any medium, provided the original work is properly cited, the use is non-commercial and no modifications or adaptations are made.

© 2022 The Authors. *European Journal of Neuroscience* published by Federation of European Neuroscience Societies and John Wiley & Sons Ltd.

**KEYWORDS**

central nervous system injury, mice, microglia, neutrophils

## 1 | INTRODUCTION

Injuries of the upper spinal cord induce a permanent loss of function caused by the axotomy of spinal pathways. This primary injury results in a cascade of inflammatory processes leading to the activation and recruitment of immune cells at and around the site of injury (Bradbury & Burnside, 2019; Hawthorne & Popovich, 2011). This includes activation of resident macrophages called microglia (Kroner & Rosas Almanza, 2019), recruitment of circulating neutrophils (Zivkovic et al., 2021), inflammatory monocytes and monocyte-derived macrophages (MDMs) (Milich et al., 2019).

Microglia are myeloid cells found in the central nervous system that clear dead and surplus cells in healthy organisms (Prinz et al., 2019). Microglia that survive the initial spinal cord injury are activated within minutes following injury (Donnelly & Popovich, 2008). They consequently proliferate and adopt an amoeboid form at the site of injury, making them difficult to distinguish from infiltrating MDMs recruited to the lesion site (Kigerl et al., 2009; Popovich et al., 2002; Rabchevsky & Streit, 1998; Subhramanyam et al., 2019). Microglia activation leads to the retraction of their processes and the secretion of inflammatory cytokines and chemokines. This secretion attracts other immune cells to the injured area to help restore cellular and molecular homeostasis (Gensel & Zhang, 2015). Following spinal cord injury, activated microglia remain indefinitely at the injured site and primarily display a proinflammatory profile during the chronic phase (Donnelly & Popovich, 2008; Kigerl et al., 2009).

Neutrophils are the first immune cells recruited after spinal cord injury, mobilizing at the area of injury in the course of hours to days and peaking around 24 h post-injury (Donnelly & Popovich, 2008; Popovich & Jones, 2003). They are attracted to the lesion site by proinflammatory chemokines and cytokines produced by resident and newly recruited cells, which detect danger-associated molecular patterns following the initial trauma (Zivkovic et al., 2021). The role of recruited neutrophils is principally degranulation and phagocytosis at the lesion site (Zivkovic et al., 2021). These neutrophils also secrete cytokines to recruit other immune cells from circulation and release proteases and oxidative enzymes involved in tissue damage, including reactive oxygen species (ROS) and

myeloperoxidase (MPO) (Nguyen et al., 2007; Noble et al., 2002; Orr & Gensel, 2018).

Extracellular traps (ETs) formation was first described in 2004 as an antimicrobial function of neutrophils (Brinkmann et al., 2004). These neutrophil extracellular traps (NETs) are primarily composed of decondensed chromatin, histones and granular enzymes such as MPO and neutrophil elastase. ETs formation has since been demonstrated in monocytes and MDMs (Aulik et al., 2012; Doster et al., 2018; Weng et al., 2022). In vivo, ETs are involved in pathogen clearance, and their antimicrobial properties are used for host defence against it (Papayannopoulos, 2017). However, in some pathologies, ETs have been demonstrated to be involved in tissue damage due to their inappropriate persistence, overexpression and aggregation (Guglietta et al., 2016; Nomura et al., 2019; Novotny et al., 2020). It has also been shown that NETs exacerbate neurological deficits in a preclinical model of traumatic brain injury (Vaibhav et al., 2020). Recently, the presence of ETs has been observed in rat spinal cord following thoracic compression (Feng et al., 2021) but without a clear identification of the cells producing these traps. Indeed, MPO positive cell can be expressed not only by neutrophils as suggested but also by other cell types such as microglia (Agrawal et al., 2021), macrophages (Boe et al., 2015; Gurski & Dittel, 2022) and monocytes (Gurski & Dittel, 2022). Interestingly, the inhibition of these ETs led to some functional recovery in the rats and a reduction in neuroinflammatory processes, suggesting a detrimental role of ETs following spinal cord injury.

The formation of microglia ETs (MiETs) has been reported in vitro and in a preclinical model of *Listeria* infection but has never been demonstrated in the spinal cord. Moreover, the implication of neutrophils in ETs formation remains unclear in the context of spinal cord injury. We therefore hypothesized that resident microglia and recruited neutrophils could both form ETs acutely, that is, at 1-day post-injury (P.I.), following cervical spinal cord injury.

## 2 | MATERIALS AND METHODS

### 2.1 | Ethics statement

Adult Swiss male mice (Janvier, France;  $n = 35$ , 30–35 g, 8-weeks old) were used in this study. The Ethics Committee

of the University of Versailles Saint-Quentin-en-Yvelines approved this study, and all experiments complied with French and European laws regarding animal experimentation (EU Directive 2010/63/EU) (Apafis #2021080910063249\_v3). The animals were housed in individual ventilated cages in a state-of-the-art animal care facility (2CARE animal facility, accreditation A78-322-3, France) with access to food and water ad libitum on a 12-hour light/dark cycle. Animals were separated in three groups: Control, Sham and 1d P.I.

## 2.2 | Second cervical (C2) spinal cord lateral hemisection surgery

To investigate ET formation after spinal cord injury, a preclinical model was produced by performing C2 spinal cord lateral hemisection surgery on adult Swiss male mice ( $n = 16$ ) (Michel-Flutot et al., 2021). Animals were anaesthetized with isoflurane (5% in 100% O<sub>2</sub>) in a closed chamber. Anaesthesia was maintained throughout the procedure (1.5%–2% isoflurane in 100% O<sub>2</sub>) through a nose cone. Animals were placed on a heating pad, and the skin and muscles above the first vertebrae were retracted. A laminectomy and a durotomy were performed at the C2 spinal cord segment. Microscissors were used to ventro-laterally hemisect the spinal cord caudal to the C2 dorsal roots, then a microscalpel was used to ensure the sectioning of all remaining fibres. The wounds and the skin were sutured closed. 1d Sham mice ( $n = 9$ ) underwent the same procedures without hemisection. The isoflurane vaporizer was then turned off, and mice received subcutaneous injections of analgesic: buprenorphine, 375 µg/kg (Buprecare from Axience, Pantin, France) and antibiotics (40 mg/kg trimethoprim and 200 mg/kg sulphadoxine: Borgal 24%, from Virbac, Carros, France).

## 2.3 | Flow cytometry

At 1-day post-surgery, mice (Control:  $n = 8$ ; Sham:  $n = 7$ ; 1d P.I.:  $n = 8$ ) were anaesthetized using 5% isoflurane in 100% O<sub>2</sub> for induction. Anaesthesia was maintained (2.5% in 21% O<sub>2</sub> balanced) through a nose cone. The left carotid was then cannulated, and animals were euthanized and perfused with 30 ml of 20 mM ethylenediaminetetraacetic acid (EDTA, BP2482-1, Thermo Fisher Scientific, Waltham, MA, USA) in phosphate-buffered saline (PBS, BP399-1, Thermo Fisher Scientific) 1X. The C1–C3 spinal cord was then dissected out and placed in collagenase D (2.5 mg/ml in (Roswell Park Memorial Institute) RPMI medium 1640, 21875-034, Thermo Fisher Scientific), cut into small pieces with microscissors and digested in an incubator (5% CO<sub>2</sub>) for 20 min at 37°C. Spinal cord samples were passed through a nylon mesh (100 µm pore size) in a 50 ml tube using RPMI as rinsing medium to obtain cell suspensions. Cells were washed for 5 min at 1500 rpm at room temperature (RT). The supernatant was eliminated, and the pellet was resuspended in 1 ml of PBS 1×. 3 × 200 µl of cell suspension was transferred to a 96-well plate (650 185, Greiner bio-one, Les Ulis, France). Cells were centrifugated for 2 min at 2000 rpm at RT. Cells were then incubated for 5 min at RT in 100 µl/well of a mix composed of Fixable Viability Dye eFluor™ 780 (1/2000, 65-0865-18, Invitrogen, Waltham, MA, USA) and SYTOX™ Green Nucleic Acid Stain (1/40000, S7020, Invitrogen, Waltham, MA, USA) in PBS 1×. One hundred microliters of PBS 1× was added in each well, and the plate was centrifugated for 2 min at 2000 rpm at RT. Cells were then incubated for 30 min at 4°C in 25 µl/well with a panel of antibodies conjugated to a fluorophore (Table 1) in PBS 1× and directed against the following markers: CD45 (30-F11), CD11b (M1/70), IA/IE (M5/114.15.2), Ly6C (HK1.4), Ly6G (1A8), citrullinated (R2 + R8 + R17) histone H3 (H3cit) and myeloperoxidase (8F4; MPO). One hundred fifty microliters of PBS 1× was

TABLE 1 List of fluorochrome-coupled antibodies used for flow cytometry analysis

Marker	Fluorochrome	Reference
CD45	Brilliant Violet 510	103138, BioLegend
CD11b	Pacific Blue	101223, BioLegend
IA/IE	Alexa Fluor 700	107621, BioLegend
Ly6C	PerCp	128011, BioLegend
Ly6G	PECy7	127617, BioLegend
Citrullinated histone H3	Alexa Fluor 594	ab5103, Abcam
MPO	PE	HM1051PE-100, Hycult Biotech

Note: BioLegend is from San Diego, CA, USA. Abcam is from Cambridge, UK. Hycult Biotech is from Uden, The Netherlands. Abbreviation: MPO, myeloperoxidase.

added in each well, and the plate was centrifugated for 2 min at 2000 rpm at RT. To properly interpret flow cytometry data, fluorescence minus one (FMO) was realized as controls for H3cit, MPO and SYTOX (Control ( $n = 2$ ), 1d Sham ( $n = 2$ ) and 1d P.I. ( $n = 2$ ) supplemental animals were used for this last experiment) (Figure S1). Cells were resuspended in PBS  $1\times$  before acquisition on a BD LSRFortessa™ III (BD Life Sciences, Franklin Lakes, NJ, USA). Analysis was performed using FlowJo™ v10.8.1 Software (BD Life Sciences, Franklin Lakes, NJ, USA).

## 2.4 | Immunohistochemistry

Animals (1d P.I.:  $n = 6$ ) were anaesthetized using 5% isoflurane in 100% O<sub>2</sub> for induction. Anaesthesia was maintained (2.5% in 21% O<sub>2</sub> balanced) through a nose cone. Mice were then euthanized by intracardiac perfusion of heparinized 0.9% NaCl (10 ml), followed by Antigenfix solution (DIAPATH, Martinengo [BG], Italy) for tissue harvesting. After perfusion, the C1–C3 spinal cord was carefully dissected and stored at 4°C in fixative for 24 h. After fixation, tissues were cryo-protected for 48 h in 30% sucrose (in 0.9% NaCl) and stored at –80°C. Frozen longitudinal (C1–C3 spinal cord) free-floating sections (30 µm) were cut using a cryostat (NX70, Thermo Fisher Scientific, Waltham, MA, USA). C1–C3 sections were stored in a cryoprotectant solution (Sucrose 30% (Pharmagrade, 141621, AppliChem, Darmstadt, Germany), ethylene glycol 30% (BP230-4, Fisher Scientific, Illkirch, France) and polyvinylpyrrolidone 40 (PVP40-100G, Sigma-Aldrich, Darmstadt, Germany) 1% in PBS  $1\times$ ) at –22°C. For immunofluorescence experiments, free-floating transverse sections of the C3–C6 spinal cord were washed and incubated 12 h in citrate buffer solution (antigen retrieval). After washing, sections were placed in blocking solution (normal donkey serum [NDS] 5% in PBS  $1\times$ ) for 30 min and then incubated with primary antibodies directed against histone H3 (citrulline R2 + R8 + R17) (rabbit, 1/100, ab5103, Abcam, Cambridge, UK), Ly6G (1A8, rat, 1/100, 127601, BioLegend, San Diego, CA, USA) and Iba1 (goat, 1/400, ab5076, Abcam, Cambridge, UK) in blocking solution (NDS 5%) 12 h on an orbital shaker at RT. After several PBS  $1\times$  washes, sections were incubated with secondary antibodies linked to the fluorochromes Alexa Fluor 488 (donkey anti-rat, 1/2000, A21208, Invitrogen, Waltham, MA, USA), Alexa Fluor 594 (donkey anti-rabbit, 1/2000, A21207, Invitrogen, Waltham, MA, USA) and Alexa Fluor 647 (donkey anti-goat, 1/2000, A21447, Invitrogen, Waltham, MA, USA) for 2 h at RT, then washed again with PBS. Images of the different sections were captured with a Hamamatsu ORCA-R<sup>2</sup> camera

mounted on an Olympus IX83 P2ZF microscope (Tokyo, Japan). Images were analyzed using ImageJ 1.53n software (National Institutes of Health, Bethesda, MD, USA).

## 2.5 | Experimental design and statistical analysis

All data were presented as mean  $\pm$  SD. Prior to any procedures or testing, animals were randomized to one of three groups as defined previously: Control, 1d Sham or 1d P.I. groups. For mean fluorescence intensity (MFI) analyses, 1d Sham and 1d P.I. values were normalized to the Control group (value = 1). For the Control group, two Control animals were included in each experiment, and the mean of the values from each animal was set to 1. A one sample *t* test was used to compare Control ( $n = 8$ ) and 1d Sham values ( $n = 7$ ), and a Student *t* test was used to compare 1d Sham ( $n = 7$ ) and 1d P.I. ( $n = 8$ ) values. For the number of microglia and neutrophils per C1–C3 spinal cord segment and the frequency of their coexpression of H3cit, MPO and SYTOX, a Student *t* test or Mann–Whitney rank sum test (when normality test or variance test failed) was used to compare the Control ( $n = 8$ ) versus 1d Sham ( $n = 7$ ) and the 1d Sham versus 1d P.I. ( $n = 8$ ) groups. For the coexpression of H3cit, MPO and SYTOX in microglia, the threshold was set to between 0% and 0.60% of cells coexpressing ET markers for the Control group, and then this threshold was applied for analysis on 1d Sham and 1d P.I. groups. For the coexpression of H3cit, MPO and SYTOX in neutrophils, the threshold was set to between 0% and 2% of cells coexpressing ET markers for the Control group, and then this threshold was applied for analysis on 1d Sham and 1d P.I. groups. For the expression of H3cit in microglia by immunofluorescence on C1–C3 spinal cord longitudinal sections ( $n = 6$  1d P.I. mice), two way repeated measures ANOVA was used to compare the differences between the injured and non-injured sides and between 300 µm width rectangular subsections. Results were considered statistically significant when  $p < 0.05$ . SigmaPlot 12.5 software (Systat Software, San Jose, CA, USA) was used for all analyses.

## 3 | RESULTS

### 3.1 | Effect of C2 spinal cord hemisection on the production of ETs by living resident microglia

Microglia residing in the central nervous system are activated within the minutes following a spinal cord injury.

We used flow cytometry to evaluate the formation of ETs by these resident microglia at 1 day following injury at the C2 section of the spinal cord. Microglia were identified as CD11b<sup>+</sup>CD45<sup>int</sup> cells (Figures 1a and S2). The absolute number of microglia was significantly lower in 1d Sham compared with Control mice ( $2217 \pm 823$  vs.  $3600 \pm 1073$  per C1–C3 spinal cord segment respectively,  $p = 0.016$ ). This number also differed between 1d Sham and 1d P.I. groups, though not to a statistically significant extent ( $1459 \pm 880$  per C1–C3 spinal cord segment in 1d P. I group,  $p = 0.110$ ) (Figure 1b). The expression of three individual known markers of ETs in microglia was investigated: citrullinated histone H3

(H3cit), which is involved in chromatin decondensation; myeloperoxidase (MPO), a granular enzyme; and SYTOX, a DNA intercalating agent. Expression of these markers was increased in 1d Sham compared with Control mice. Expression of H3cit was  $1.63 \pm 0.36$  AU versus 1 AU,  $p = 0.003$  (Figure 1c). Expression of MPO was  $1.16 \pm 0.07$  AU versus 1 AU,  $p < 0.001$  (Figure 1d). Expression of SYTOX was  $1.39 \pm 0.27$  AU versus 1 AU,  $p = 0.009$  (Figure 1e). This increased expression was further amplified in 1d P.I. mice (H3cit:  $2.66 \pm 0.49$  AU,  $p < 0.001$ ; MPO:  $2.14 \pm 0.54$  AU,  $p < 0.001$ ; SYTOX:  $2.72 \pm 0.50$  AU,  $p < 0.001$ ) compared with 1d Sham animals (Figure 1c–e).

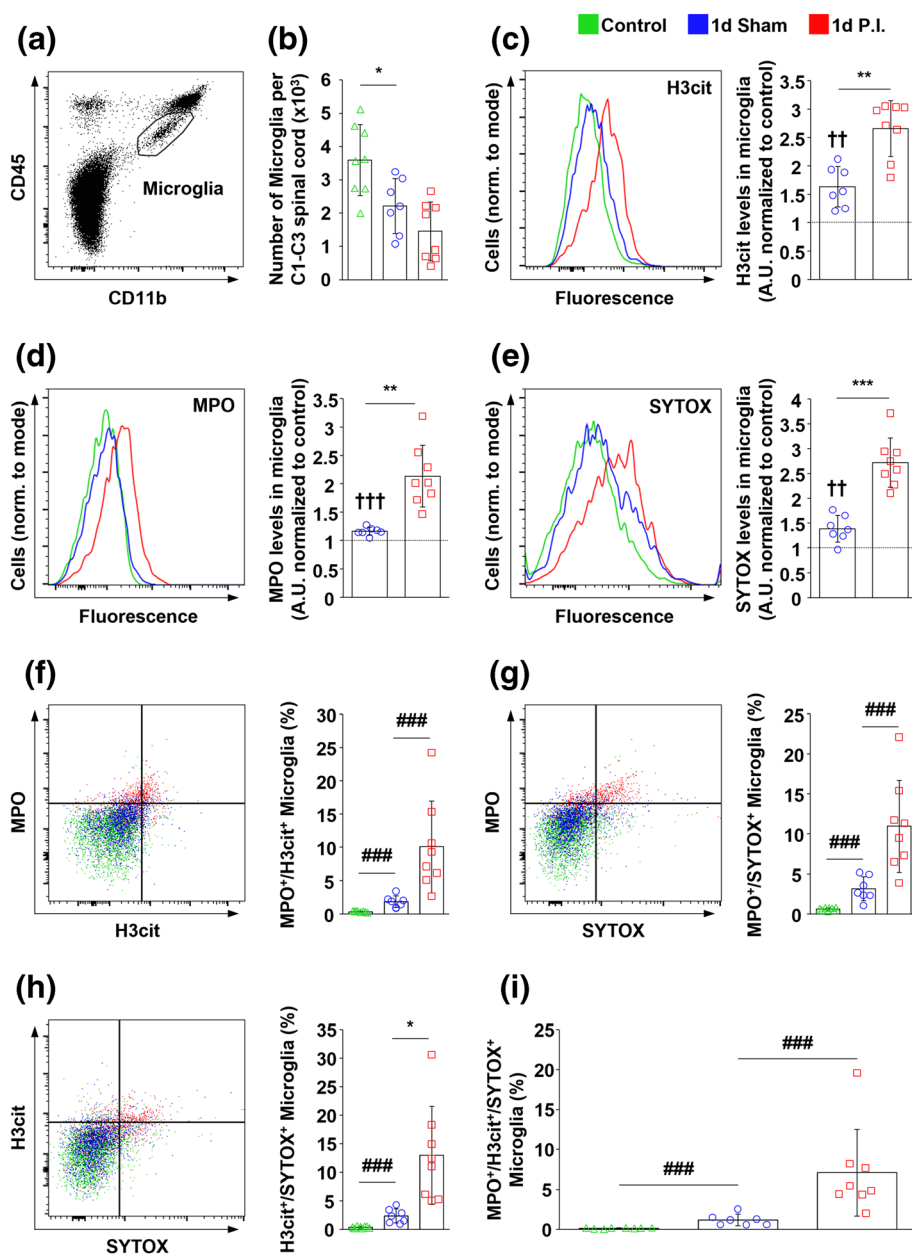


**FIGURE 1** Microglia extracellular traps formation following a C2 spinal cord injury in 1-day post-injury (1d P.I.) mice. (a) Representative gating of CD45<sup>int</sup>CD11b<sup>+</sup> living microglia from the C1 to C3 spinal cord segment of a 1d P.I. mouse. (b) Number of microglia per C1–C3 spinal cord segment in Control (green), 1d Sham (blue) and 1d P.I. (red) groups. (c, d, e) Representative histogram and corresponding expression of citrullinated histone H3 (H3cit) (c), myeloperoxidase (MPO) (d) and SYTOX (e) in Control (green), 1d Sham (blue) and 1d P.I. (red) groups. 1-d Sham and 1d P.I. animal values have been normalized to the values of control animals (dotted line at 1 U.A.). (f, g, h) Representative dot plot and corresponding percentage of living microglia co-expressing MPO and H3cit (f), MPO and SYTOX (g) and H3cit and SYTOX (h) in Control (green), 1d Sham (blue) and 1d P.I. (red) groups. (i) Percentage of living microglia co-expressing MPO, H3cit and SYTOX in Control (green), 1d Sham (blue) and 1d P.I. (red) groups. \* $p < 0.05$ ; Student *t* test. \*\* $p < 0.001$ ; Student *t* test. \*\*\* $p < 0.0001$ ; Student *t* test. †† $p < 0.01$ ; compared with Control group, two-tailed one-sample *t* test. ††† $p < 0.001$ ; compared with Control group, two-tailed one-sample *t* test. ### $p \leq 0.001$ ; Mann–Whitney rank sum test

### 3.2 | Colocalization of ETs markers in resident microglia

Our results display individual expression levels of H3cit, MPO and SYTOX. However, the coexpression of these ETs markers is a better proxy for ET formation, considering that an increased expression of MPO alone, for instance, could alternatively reflect cell degranulation. We therefore additionally evaluated the frequency of microglia coexpression of H3cit/MPO, SYTOX/MPO and SYTOX/H3cit. The C2 spinal cord hemisection induced a dramatic increase in the frequency of microglia coexpressing these markers in 1d P.I. mice (H3cit/MPO:  $10.04 \pm 6.89\%$ ; SYTOX/MPO:  $12.96 \pm 8.58\%$ ; SYTOX/H3cit:  $10.95 \pm 5.74\%$ ) compared with 1d Sham mice (H3cit/MPO:  $1.81 \pm 0.88\%$ ,  $p < 0.001$ ; SYTOX/MPO:  $2.37 \pm 1.25\%$ ,  $p < 0.001$ ; SYTOX/H3cit:  $3.14 \pm 1.50\%$ ,  $p = 0.004$ ) (Figure 1f–h). Interestingly, coexpression was also increased in the 1d Sham group compared with the Control group (H3cit/MPO:  $0.32 \pm 0.11\%$ ,  $p < 0.001$ ; SYTOX/MPO:  $0.39 \pm 0.19\%$ ,  $p < 0.001$ ; SYTOX/H3cit:  $0.60 \pm 0.17\%$ ,  $p < 0.001$ ) (Figure 1f–h). Furthermore, the coexpression of all three markers was evaluated. A significant increase in the frequency of microglia cells coexpressing H3cit, MPO and SYTOX was observed in 1d P.I. mice ( $7.07 \pm 5.42\%$ ) compared with 1d Sham mice ( $1.18 \pm 0.71\%$ ,  $p < 0.001$ ) (Figure 1i). A significant increase was likewise observed in the 1d Sham group compared with the Control group ( $0.12 \pm 0.05\%$ ;  $p < 0.001$ ) (Figure 1i).

### 3.3 | Prediction of ETs production by microglia in the C1–C3 injured spinal cord

Evaluation of ET production in fixed tissue sections is frequently evaluated by quantification of the H3cit in cells. Quantification of H3cit serves as a proxy not only for cells producing ETs but also for cells on the verge of producing ETs. In this study, we quantified the expression of H3cit in identified microglia (Iba1+ cells) in the 1d injured spinal cord to confirm MiET production across tissue sections (Figure 2a). On the injured side, H3cit expression was significantly higher in segments between 0 and 300  $\mu\text{m}$  rostrally ( $43.72 \pm 6.25$  AU) compared with more rostral segments, that is, between 300 and 600  $\mu\text{m}$  ( $32.49 \pm 6.11$  AU,  $p < 0.001$ ) and between 600 and 900  $\mu\text{m}$  ( $30.28 \pm 5.03$  AU,  $p < 0.001$ ). Similarly, the expression of H3cit was significantly higher in segments between 0 and 300  $\mu\text{m}$  caudally ( $48.93 \pm 14.31$  AU) compared with more caudal segments, that is, between 300 and 600  $\mu\text{m}$  ( $34.44 \pm 6.51$  AU,  $p < 0.001$ ), and between 600 and 900  $\mu\text{m}$  ( $28.86 \pm 6.14$  AU,  $p < 0.001$ ) (Figure 2b). Conversely, this

expression did not vary significantly between the different segments of the intact side ( $p > 0.05$ ). We then compared the expression of H3cit in microglia between the injured and the intact sides. At the level of the injury, this expression was significantly increased in the injured side compared with the intact side rostrally between 0 and 300  $\mu\text{m}$  from the injured area ( $26.82 \pm 5.16$  AU,  $p < 0.001$ ) and caudally between 0 and 300  $\mu\text{m}$  ( $26.79 \pm 4.41$  AU,  $p < 0.001$ ) and between 300 and 600  $\mu\text{m}$  ( $26.15 \pm 4.58$  AU,  $p = 0.022$ ) from the injured area (Figure 2b). These results suggest that microglia located near the injury site are most likely to form ETs, in agreement with our flow cytometry results. These microglia express higher nuclear H3cit labelling compared with more distal microglia (Figure 2b,c). Note the clear deposition of H3cit labelling at the border around the lesion site (Figure 2a), which likely represents the separation between the viable tissue and a zone of necrosis as described in other pathologies.

Taken together, these results display that after a durotomy, resident microglia produce ETs, and this production is increased following spinal cord injury particularly in tissue closest to the injury site.

### 3.4 | Effect of C2 spinal cord injury on the recruitment of neutrophils and the production of markers of NETs

Neutrophils are the first peripheral immune cells to be recruited to the injured site following spinal cord injury. The formation of ETs by neutrophils (NETs) is well-described in other organs and models (Boettcher et al., 2020; Li & Tablin, 2018; Nomura et al., 2019), leading us to wonder if infiltrating neutrophils could form ETs in the injured spinal cord. Neutrophils have been identified as CD11b<sup>+</sup>CD45<sup>high</sup>Ly6G<sup>+</sup> cells (Figures 3a and S2). In agreement with findings of other studies (Donnelly & Popovich, 2008), absolute number of neutrophils was increased in the C1–C3 spinal cord at 1 day following C2 spinal cord hemisection ( $3255 \pm 1878$  per C1–C3 spinal cord segment) compared with 1d Sham group ( $251 \pm 141$  vs.  $70 \pm 37$  per C1–C3 spinal cord segment,  $p < 0.001$ ; Figure 3i). Interestingly, the durotomy performed in the 1d Sham group also led to an increase in infiltrating neutrophils compared with the Control group ( $70 \pm 37$  per C1–C3 spinal cord segment,  $p = 0.002$ ). As with microglia, we measured neutrophil H3cit, MPO and SYTOX expression using flow cytometry. A significant increase in H3cit expression was observed in the 1d Sham group ( $1.64 \pm 0.32$  AU) compared with the Control group (1 AU,  $p = 0.002$ ; Figure 3b). There was no difference in MPO expression between the

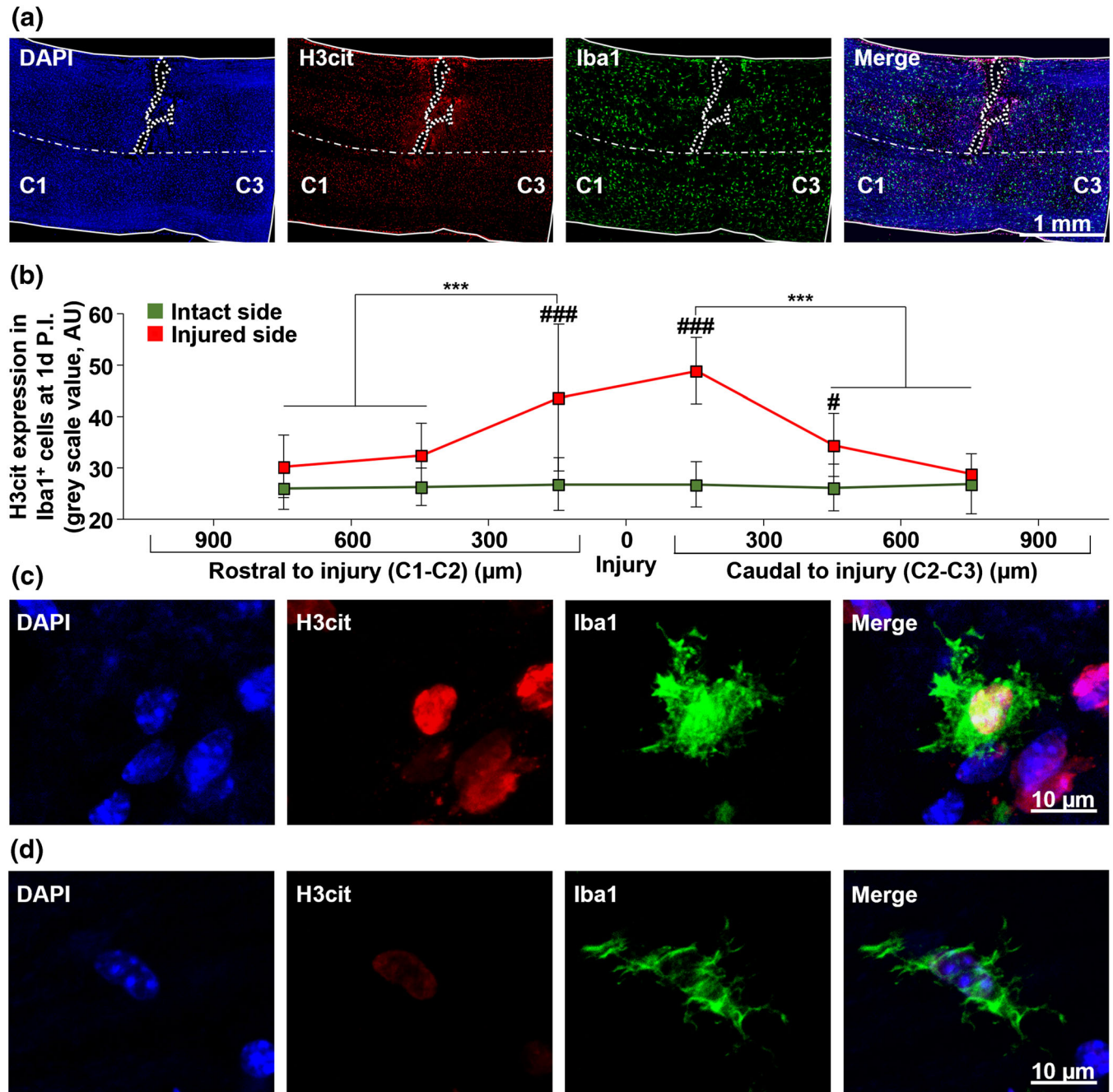


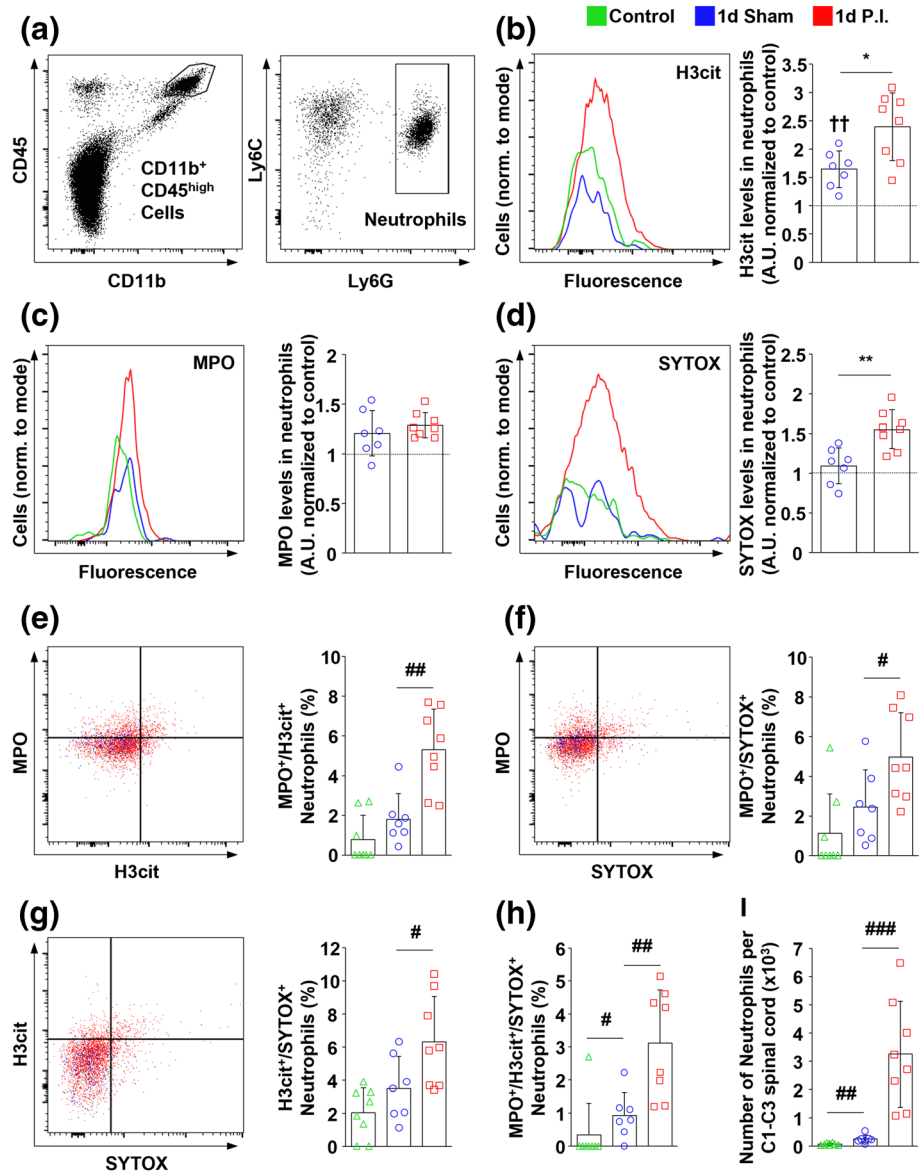
**FIGURE 2** H3cit expression in microglia following a C2 spinal cord injury in 1-day post-injury (1d P.I.) mice. (a) Representative pictures of Iba1<sup>+</sup> microglia in green expressing citrullinated histone H3 (H3cit, red) from the C1 to C3 spinal cord segment of a 1d P.I. mouse. The nucleus of cells is labelled with 4',6-diamidino-2-phenylindole (DAPI) in blue. The spinal cord is delineated with the white solid line, the median is delineated with the white dashed line and the injury area is contoured with the white dotted line. (b) Expression of H3cit for the intact side (green line) and the injured side (red line) depending on distance to the site of injury. (c) Representative pictures, showing a magnified microglia near the site of injury, from panel (a). (d) Representative pictures, showing a magnified microglia far from the site of injury (caudal part), from panel (a). \*\*\* $p < 0.001$ ; injured side versus intact side from 0 to 300  $\mu\text{m}$  rostral and caudal to injury, two way repeated measures ANOVA. # $p = 0.022$ ; injured side versus intact side from 300 to 600  $\mu\text{m}$  caudal to injury, two way repeated measures ANOVA. \*\*\* $p < 0.001$ ; 0 to 300  $\mu\text{m}$  rostral versus 300 to 600  $\mu\text{m}$ , 600 to 900  $\mu\text{m}$  and 900 to 1200  $\mu\text{m}$  rostral to injury, two way repeated measures ANOVA

Control and 1d Sham groups (1 AU vs.  $1.21 \pm 0.23$  AU, respectively,  $p = 0.051$ ; Figure 3c) or SYTOX expression between the Control and 1d Sham groups (1 AU vs. 1.10

$\pm 0.23$  AU, respectively,  $p = 0.31$ ; Figure 3d). The increased H3cit expression was amplified in 1d P.I. mice ( $2.39 \pm 0.60$  AU,  $p = 0.011$ ) compared with 1d Sham



**FIGURE 3** Neutrophil extracellular traps formation following a C2 spinal cord injury in 1-day post-injury (1d P.I.) mice. (a) Representative gating of CD45<sup>high</sup>CD11b<sup>+</sup>Ly6C<sup>+</sup>Ly6G<sup>+</sup> living neutrophils from the C1 to C3 spinal cord segment of a 1d P.I. mouse. (b, c, d) Representative histogram and corresponding expression of citrullinated histone H3 (H3cit) (b), myeloperoxidase (MPO) (c) and SYTOX (d) in Control (green), 1d Sham (blue) and 1d P.I. (red) groups. 1d Sham and 1d P.I. animal values have been normalized to the values of Control animals (dotted line at 1 U.A.). (e, f, g) Representative dot plot and corresponding percentage of living neutrophils co-expressing MPO and H3cit (e), MPO and SYTOX (f) and H3cit and SYTOX (g) in Control (green), 1d Sham (blue) and 1d P.I. (red) groups. (h) Percentage of living neutrophils co-expressing MPO, H3cit and SYTOX in Control (green), 1d Sham (blue) and 1d P.I. (red) groups. (i) Number of living neutrophils per C1–C3 spinal cord segment in Control (green), 1d Sham (blue) and 1d P.I. (red) groups. \* $p < 0.05$ ; Student  $t$  test. \*\* $p < 0.01$ , Student  $t$  test. †† $p < 0.01$ ; compared with Control group, two-tailed one-sample  $t$  test. # $p < 0.05$ ; Mann–Whitney rank sum test. ## $p < 0.01$ ; Mann–Whitney rank sum test. ### $p \leq 0.001$ ; Mann–Whitney rank sum test



mice (Figure 2b). An increase in SYTOX expression was also observed in 1d P.I. mice ( $1.55 \pm 0.24$  AU) compared with 1d Sham mice ( $p = 0.002$ ; Figure 3d). No difference in MPO expression was observed between the 1d P.I. ( $1.29 \pm 0.13$  AU) and 1d Sham groups ( $p = 0.41$ ; Figure 3c).

### 3.5 | Colocalization of ETs markers in infiltrating neutrophils

We evaluated the changes in the frequency of neutrophils coexpressing H3cit/MPO, SYTOX/MPO and SYTOX/H3cit. There was no significant difference between the Control and 1d Sham groups in the percentage of neutrophils coexpressing H3cit/MPO ( $0.79 \pm 1.21\%$  vs.  $1.81 \pm 1.28\%$ , respectively,  $p = 0.094$ ; Figure 3e),

SYTOX/MPO ( $1.13 \pm 1.97\%$  vs.  $2.45 \pm 1.87\%$ , respectively,  $p = 0.094$ ; Figure 3f) and SYTOX/H3cit ( $2.03 \pm 1.49\%$  vs.  $3.49 \pm 1.94\%$ , respectively,  $p = 0.125$ ; Figure 3g). The C2 spinal cord hemisection, however, induced an increased coexpression of these markers in 1d P.I. mice (H3cit/MPO:  $5.30 \pm 2.04\%$ ,  $p = 0.002$ ; SYTOX/MPO:  $4.95 \pm 2.24\%$ ,  $p = 0.037$ ; SYTOX/H3cit:  $6.30 \pm 2.76\%$ ,  $p < 0.043$ ) compared with 1d Sham mice (Figure 3f–h). We also assessed the percentage of neutrophils coexpressing all three markers. The percentage of neutrophils expressing H3cit, MPO and SYTOX was significantly higher in the 1d P.I. group ( $3.11 \pm 1.62\%$ ) compared with the 1d Sham group ( $0.92 \pm 0.70\%$ ,  $p = 0.002$ ; Figure 3h). The durotomy in 1d Sham mice also led to an increase in neutrophils expressing all three markers compared with Control mice ( $0.34 \pm 0.96\%$ ,  $p = 0.040$ ; Figure 3h).

### 3.6 | Neutrophil localization and H3cit expression

Finally, we observed the presence and location of infiltrating neutrophils in the injured spinal cord. We found that these neutrophils are located around the lesion site (Figure 4a). Among these neutrophils, some presented a strong H3cit labelling (Figure 4b) whereas others presented a weaker H3cit labelling (Figure 4c). Taken together, these results display that after spinal cord injury, infiltrating neutrophils produce ETs at the site of injury.

## 4 | DISCUSSION

In the present study, we demonstrated the involvement of resident microglia and infiltrating neutrophils in the formation of ETs in the spinal cord following injury. To date, the formation of ETs has been reported in neutrophils (Brinkmann et al., 2004), monocytes (Webster et al., 2010), MDMs (Boe et al., 2015) and more recently, in microglia (Wang et al., 2019). However, the formation of ETs by these specific cells was never observed in spinal cord. At 1-day P.I., activated microglia and infiltrating neutrophils are fully present at the injured site in rodents, but monocytes and MDMs do not invade the

injury area until later (Donnelly & Popovich, 2008). To identify these cells, Ly6G marker for neutrophils and Iba1 for microglia (Sasaki et al., 2001) were used in immunostaining and gated as  $CD11b^{+}CD45^{high}Ly6G^{+}$  cells and  $CD11b^{+}CD45^{int}$  cells, respectively, in flow cytometry (Figure S1). Our results indicate that resident microglia and infiltrating neutrophils form ETs soon (1 day) after a spinal cord injury. More specifically, these ETs can be considered vital ETs, meaning leading to release of ETs in the extracellular space without compromising cell survival (Papayannopoulos, 2017). This is compared with suicidal ETs, formation of which leads to membrane permeabilization and cell death. In this study, we evaluated ET formation only in living cells by flow cytometry, but this does not exclude the presence of suicidal ETs.

By immunolabelling, we observed an increase of H3cit expression in microglia around the lesion site, as well as in some of the infiltrating neutrophils (Figures 2 and 4). This correlates with our cytometry results showing that not all microglia and neutrophils increase their expression of markers of ET formation. However, it remains to be determined if suicidal ETs formation also occurs, what might be the ratio of vital and suicidal ETs in microglia and neutrophils, as well as the timing and the duration of ETs formation following spinal cord injury. We also did not evaluate whether invading MDMs

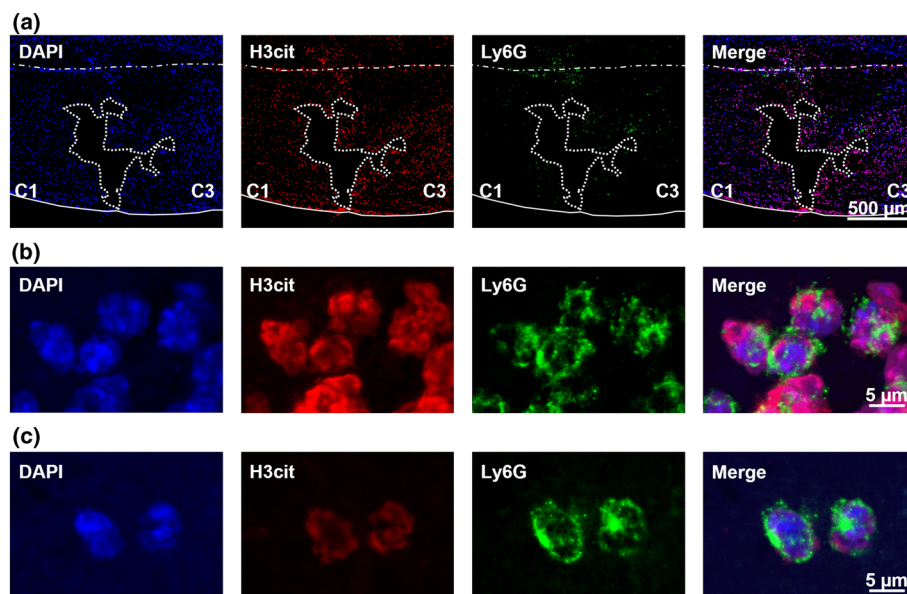


**FIGURE 4** Presence of neutrophils expressing H3cit at the site of injury following a C2 spinal cord injury in 1-day post-injury (1d P.I.) mice. (a) Representative pictures of  $Ly6G^{+}$  neutrophils in green and labelling of citrullinated histone H3 (H3cit) in red from the C1 to C3 spinal cord segment of a 1d P.I. mouse. The nucleus of cells is labelled with 4',6-diamidino-2-phenylindole (DAPI) in blue. The spinal cord is delineated with the white solid line, the median is delineated with the white dashed line and the injury area is contoured with the white dotted line. (b) Representative pictures, showing magnified neutrophils expressing high levels of H3cit, from panel (a). (c) Representative pictures, showing magnified neutrophils expressing low levels of H3cit, from panel (a)

also participate in ET formation. A study of the kinetics of NET, MiET and macrophage ET (MET) production could lead to a better understanding of the role of these ETs in the neuroinflammatory processes following spinal cord injury. However, precautions must be taken in kinetic evaluation. Activated microglia adopt an amoeboid form and upregulate markers also expressed by MDMs, which make them hardly distinguishable from infiltrating MDMs by immunolabelling and flow cytometry (Kroner & Rosas Almanza, 2019). More specifically, activated microglia upregulate their expression of CD45 and become CD11b<sup>+</sup>CD45<sup>high</sup>, like MDMs (Martin et al., 2017). This could explain the reduction in the number of microglia observed in our 1d Sham animals compared with the Control group, and the similar number observed between the 1d Sham and 1d P.I. groups. Perhaps some microglia became CD11b<sup>+</sup>CD45<sup>high</sup> and were excluded from microglia gating (Cosenza-Nashat et al., 2006). It is likely these microglia have a higher level of activation than gated microglia and therefore could produce MiETs as CD11b<sup>+</sup>CD45<sup>int</sup>. To solve this problem of identification, transgenic mice produced by crossbreeding would allow expression of a fluorescent molecule under CX3CR1 promoter, which is tamoxifen-inducible. MDMs, which have a quicker turnover than microglia, would lose their fluorescence, leaving only microglia labelled (Yona et al., 2013). This study design would facilitate further study of ETs produced specifically by microglia and MDMs after spinal cord injury.

We also observed that living microglia and neutrophils increase their ET formation following durotomy. This result correlates with other studies demonstrating the formation of NETs by infiltrating neutrophils in mouse models of durotomy (Jin et al., 2020). However, this is the first report of MiET formation in the spinal cord following durotomy. This phenomenon should be considered in cases of spine operation, as the occurrence of this neuroinflammatory process can result in late neurological deficits.

NETs are already known to exacerbate neurological deficits, and their inhibition using deoxyribonuclease-1 (DNase1; cleave DNA) or peptidylarginine deiminase 4 (PAD4; involved in the citrullination of histone H3) inhibitors leads to improved functional outcomes following traumatic brain (Vaibhav et al., 2020) and spinal cord injury (Feng et al., 2021). Other studies have demonstrated that administration of ET inhibitors such as neutrophil elastase inhibitor (sivelestat) induces beneficial effects following spinal cord injury but without mentioning ETs or evaluating the expression of their constituents (Kumar et al., 2018). This supports a potential harmful effect of ETs following central nervous system injury. Moreover, in cases of spinal cord injury, inhibition of ETs

leads to reduced glial scarring (Feng et al., 2021). This correlates with our immunolabelling results suggesting that microglia near the lesion site are most likely to form MiETs. The inhibition of these MiETs could indeed result in reduced neuroinflammation in this area and, consequently, reduced scar tissue formation. However, the drug administration was done immediately following the induction of the model (Feng et al., 2021; Vaibhav et al., 2020), meaning only ETs formed by microglia and infiltrating neutrophils, but not infiltrating MDM and chronically activated microglia at later time-points, were targeted. It is likely that a more defined and chronically delivered therapeutic could maximize the benefits of ET inhibition. ET-inhibiting drugs should be compared to determine the most appropriate one, as different drugs target different stages of ET formation (histone H3 citrullination, DNA, formation of pore to expel the ETs, etc.). Some of these inhibitors are under clinical trial (Chiang et al., 2020). It remains unclear how ET inhibition leads to improved functional outcome, especially following spinal cord injury. The impact of this inhibition on the inflammatory and plasticity processes that take place following injury represents a worthy research topic. This could be achieved by studying the effect of ET inhibitors on the overexpression of chondroitin sulphate proteoglycan (known to inhibit plasticity processes) (Bartus et al., 2012; Kwok et al., 2014) or on axonal sprouting or rewiring (Ballermann & Fouad, 2006; Darlot et al., 2012) and the expression of neural growth factors (Keefe et al., 2017). The potential beneficial effects of ETs should also be explored, such as ET facilitation of myelin debris clearing following injury.

To conclude, our results highlight a new role of resident microglia following spinal cord injury: the formation of MiETs. We also showed that infiltrating neutrophils produce ETs 1 day following injury. These two types of immune cells are more likely to form ETs in tissue closest to the site of injury. However, it remains unknown if more chronically infiltrating MDMs also form ETs in the injured spinal cord. We also did not evaluate the proportion of vital versus suicidal ETs and their specific roles in the pathology. To this aim, a study of the kinetics of NET, MiET and MET formation should be performed to better understand this inflammatory process and pave the way for post-injury therapies that effectively target ETs.

## ACKNOWLEDGEMENTS

This work was supported by funding from the Chancellerie des Universités de Paris (Legs Poix) (SV), INSERM (SV and AM), Université de Versailles Saint-Quentin-en-Yvelines (SV and AM) and Fondation pour la recherche médicale ECO202106013756 (AM and LE).

The supporters had no role in study design, data collection and analysis, decision to publish or preparation of the manuscript. This work has benefited from the Department of Biotechnologies of the University of Versailles Saint-Quentin en Yvelines (CYMAGES and histology facilities, UFR SVS, UVSQ, Université Paris-Saclay, 78180 Montigny-le-Bretonneux, France). We thank Lucille Adam for her precious advice. The graphical abstract includes modified templates from Servier Medical Art, provided by Servier, licensed under a Creative Commons Attribution 3.0 unported licence.

## CONFLICT OF INTEREST

None.

## AUTHOR CONTRIBUTIONS

**Pauline Michel-Flutot:** conceptualization, investigation, formal analysis, visualization, project administration, writing—original draft and review and editing. **Camille H Bourcier:** investigation and writing—review and editing. **Laila Emam:** investigation, formal analysis and writing—review and editing. **Adeline Gasser:** writing—review and editing. **Simon Glatigny:** writing—review and editing. **Stéphane Vinit:** conceptualization, methodology, supervision, project administration, funding acquisition and writing—review and editing. **Arnaud Mansart:** conceptualization, methodology, supervision, project administration, funding acquisition and writing—review and editing.

## PEER REVIEW

The peer review history for this article is available at <https://publons.com/publon/10.1111/ejn.15902>.

## DATA AVAILABILITY STATEMENT

The data presented in this study are available here: <https://1drv.ms/u/s!Auu8ZYHjFnnHhL4gAmBsDHk61EbkbQ?e=LmW5NE>.

## ORCID

Pauline Michel-Flutot  <https://orcid.org/0000-0002-5003-217X>

Stéphane Vinit  <https://orcid.org/0000-0001-7013-1741>

## REFERENCES

- Agrawal, I., Sharma, N., Saxena, S., Arvind, S., Chakraborty, D., Chakraborty, D. B., Jha, D., Ghatak, S., Epari, S., Gupta, T., & Jha, S. (2021). Dopamine induces functional extracellular traps in microglia. *iScience*, *24*(1), 101968. <https://doi.org/10.1016/j.isci.2020.101968>
- Aulik, N. A., Hellenbrand, K. M., Czaprynski, C. J., & Urban, J. F. (2012). Mannheimia haemolytica and its leukotoxin cause macrophage extracellular trap formation by bovine macrophages. *Infection and Immunity*, *80*(5), 1923–1933. <https://doi.org/10.1128/IAI.06120-11>
- Ballermann, M., & Fouad, K. (2006). Spontaneous locomotor recovery in spinal cord injured rats is accompanied by anatomical plasticity of reticulospinal fibers. *European Journal of Neuroscience*, *23*(8), 1988–1996. <https://doi.org/10.1111/j.1460-9568.2006.04726.x>
- Bartus, K., James, N. D., Bosch, K. D., & Bradbury, E. J. (2012). Chondroitin sulphate proteoglycans: Key modulators of spinal cord and brain plasticity. *Experimental Neurology*, *235*(1), 5–17. <https://doi.org/10.1016/j.expneurol.2011.08.008>
- Boe, D. M., Curtis, B. J., Chen, M. M., Ippolito, J. A., & Kovacs, E. J. (2015). Extracellular traps and macrophages: New roles for the versatile phagocyte. *Journal of Leukocyte Biology*, *97*(6), 1023–1035. <https://doi.org/10.1189/jlb.4RI1014-521R>
- Boettcher, M., Esser, M., Trah, J., Klohs, S., Mokhaberi, N., Wenskus, J., Trochimiuk, M., Appl, B., Reinshagen, K., Raluy, L. P., & Klinke, M. (2020). Markers of neutrophil activation and extracellular traps formation are predictive of appendicitis in mice and humans: A pilot study. *Scientific Reports*, *10*(1), 18240. <https://doi.org/10.1038/s41598-020-74370-9>
- Bradbury, E. J., & Burnside, E. R. (2019). Moving beyond the glial scar for spinal cord repair. *Nature Communications*, *10*(1), 3879. <https://doi.org/10.1038/s41467-019-11707-7>
- Brinkmann, V., Reichard, U., Goosmann, C., Fauler, B., Uhlemann, Y., Weiss, D. S., Weinrauch, Y., & Zychlinsky, A. (2004). Neutrophil extracellular traps kill bacteria. *Science*, *303*(5663), 1532–1535. <https://doi.org/10.1126/science.1092385>
- Chiang, C.-C., Korinek, M., Cheng, W.-J., & Hwang, T.-L. (2020). Targeting neutrophils to treat acute respiratory distress syndrome in coronavirus disease. *Frontiers in Pharmacology*, *11*, 572009. <https://doi.org/10.3389/fphar.2020.572009>
- Cosenza-Nashat, M. A., Kim, M.-O., Zhao, M.-L., Suh, H.-S., & Lee, S. C. (2006). CD45 isoform expression in microglia and inflammatory cells in HIV-1 encephalitis. *Brain Pathology (Zurich, Switzerland)*, *16*(4), 256–265. <https://doi.org/10.1111/j.1750-3639.2006.00027.x>
- Darlot, F., Cayetanot, F., Gauthier, P., Matarazzo, V., & Kastner, A. (2012). Extensive respiratory plasticity after cervical spinal cord injury in rats: Axonal sprouting and rerouting of ventrolateral bulbospinal pathways. *Experimental Neurology*, *236*(1), 88–102. <https://doi.org/10.1016/j.expneurol.2012.04.004>
- Donnelly, D. J., & Popovich, P. G. (2008). Inflammation and its role in neuroprotection, axonal regeneration and functional recovery after spinal cord injury. *Experimental Neurology*, *209*(2), 378–388. <https://doi.org/10.1016/j.expneurol.2007.06.009>
- Doster, R. S., Rogers, L. M., Gaddy, J. A., & Aronoff, D. M. (2018). Macrophage extracellular traps: A scoping review. *Journal of Innate Immunity*, *10*(1), 3–13. <https://doi.org/10.1159/000480373>
- Feng, Z., Min, L., Liang, L., Chen, B., Chen, H., Zhou, Y., Deng, W., Liu, H., & Hou, J. (2021). Neutrophil extracellular traps exacerbate secondary injury via promoting neuroinflammation and blood–spinal cord barrier disruption in spinal cord injury. *Frontiers in Immunology*, *12*, 698249. <https://doi.org/10.3389/fimmu.2021.698249>
- Gensel, J. C., & Zhang, B. (2015). Macrophage activation and its role in repair and pathology after spinal cord injury. *Brain*

- Research*, 1619, 1–11. <https://doi.org/10.1016/j.brainres.2014.12.045>
- Guglietta, S., Chiavelli, A., Zagato, E., Krieg, C., Gandini, S., Ravenda, P. S., Bazolli, B., Lu, B., Penna, G., & Rescigno, M. (2016). Coagulation induced by C3aR-dependent NETosis drives protumorigenic neutrophils during small intestinal tumorigenesis. *Nature Communications*, 7, 11037. <https://doi.org/10.1038/ncomms11037>
- Gurski, C. J., & Dittel, B. N. (2022). Myeloperoxidase as a marker to differentiate mouse monocyte/macrophage subsets. *International Journal of Molecular Sciences*, 23(15), 8246. <https://doi.org/10.3390/ijms23158246>
- Hawthorne, A. L., & Popovich, P. G. (2011). Emerging concepts in myeloid cell biology after spinal cord injury. *Neurotherapeutics*, 8(2), 252–261. <https://doi.org/10.1007/s13311-011-0032-6>
- Jin, Z., Sun, J., Song, Z., Chen, K., Nicolas, Y. S. M., Kc, R., Ma, Q., Liu, J., & Zhang, M. (2020). Neutrophil extracellular traps promote scar formation in post-epidural fibrosis. *Regenerative Medicine*, 5(1), 19. <https://doi.org/10.1038/s41536-020-00103-1>
- Keefe, K. M., Sheikh, I. S., & Smith, G. M. (2017). Targeting neurotrophins to specific populations of neurons: NGF, BDNF, and NT-3 and their relevance for treatment of spinal cord injury. *International Journal of Molecular Sciences*, 18(3), 548. <https://doi.org/10.3390/ijms18030548>
- Kigerl, K. A., Gensel, J. C., Ankeny, D. P., Alexander, J. K., Donnelly, D. J., & Popovich, P. G. (2009). Identification of two distinct macrophage subsets with divergent effects causing either neurotoxicity or regeneration in the injured mouse spinal cord. *The Journal of Neuroscience*, 29(43), 13435–13444. <https://doi.org/10.1523/jneurosci.3257-09.2009>
- Kroner, A., & Rosas Almanza, J. (2019). Role of microglia in spinal cord injury. *Neuroscience Letters*, 709, 134370. <https://doi.org/10.1016/j.neulet.2019.134370>
- Kumar, H., Choi, H., Jo, M. J., Joshi, H. P., Muttigi, M., Bonanomi, D., Kim, S. B., Ban, E., Kim, A., Lee, S. H., Kim, K. T., Sohn, S., Zeng, X., & Han, I. (2018). Neutrophil elastase inhibition effectively rescued angiopoietin-1 decrease and inhibits glial scar after spinal cord injury. *Acta Neuropathologica Communications*, 6(1), 73. <https://doi.org/10.1186/s40478-018-0576-3>
- Kwok, J. C. F., Heller, J. P., Zhao, R.-R., & Fawcett, J. W. (2014). Targeting inhibitory chondroitin sulphate proteoglycans to promote plasticity after injury. In A. J. Murray (Ed.), *Axon growth and regeneration: Methods and protocols* (pp. 127–138). Springer New York.
- Li, R. H. L., & Tablin, F. (2018). A comparative review of neutrophil extracellular traps in sepsis. *Frontiers in Veterinary Science*, 5, 291. <https://doi.org/10.3389/fvets.2018.00291>
- Martin, E., El-Behi, M., Fontaine, B., & Delarasse, C. (2017). Analysis of microglia and monocyte-derived macrophages from the central nervous system by flow cytometry. *Journal of Visualized Experiments*, (124), e55781. <https://doi.org/10.3791/55781>
- Michel-Flutot, P., Mansart, A., Deramaudt, B. T., Jesus, I., Lee, K., Bonay, M., & Vinit, S. (2021). Permanent diaphragmatic deficits and spontaneous respiratory plasticity in a mouse model of incomplete cervical spinal cord injury. *Respiratory Physiology & Neurobiology*, 284, 103568. <https://doi.org/10.1016/j.resp.2020.103568>
- Milich, L. M., Ryan, C. B., & Lee, J. K. (2019). The origin, fate, and contribution of macrophages to spinal cord injury pathology. *Acta Neuropathologica*, 137(5), 785–797. <https://doi.org/10.1007/s00401-019-01992-3>
- Nguyen, H. X., O'Barr, T. J., & Anderson, A. J. (2007). Polymorphonuclear leukocytes promote neurotoxicity through release of matrix metalloproteinases, reactive oxygen species, and TNF-alpha. *Journal of Neurochemistry*, 102(3), 900–912. <https://doi.org/10.1111/j.1471-4159.2007.04643.x>
- Noble, L. J., Donovan, F., Igarashi, T., Goussev, S., & Werb, Z. (2002). Matrix metalloproteinases limit functional recovery after spinal cord injury by modulation of early vascular events. *The Journal of Neuroscience*, 22(17), 7526–7535. <https://doi.org/10.1523/jneurosci.22-17-07526.2002>
- Nomura, K., Miyashita, T., Yamamoto, Y., Munesue, S., Harashima, A., Takayama, H., Fushida, S., & Ohta, T. (2019). Citrullinated histone H3: Early biomarker of neutrophil extracellular traps in septic liver damage. *The Journal of Surgical Research*, 234, 132–138. <https://doi.org/10.1016/j.jss.2018.08.014>
- Novotny, J., Oberdieck, P., Titova, A., Pelisek, J., Chandraratne, S., Nicol, P., Hapfelmeier, A., Joner, M., Maegdefessel, L., Poppert, H., Pircher, J., Massberg, S., Friedrich, B., Zimmer, C., Schulz, C., & Boeckh-Behrens, T. (2020). Thrombus NET content is associated with clinical outcome in stroke and myocardial infarction. *Neurology*, 94(22), e2346–e2360. <https://doi.org/10.1212/wnl.00000000000009532>
- Orr, M. B., & Gensel, J. C. (2018). Spinal cord injury scarring and inflammation: Therapies targeting glial and inflammatory responses. *Neurotherapeutics*, 15(3), 541–553. <https://doi.org/10.1007/s13311-018-0631-6>
- Papayannopoulos, V. (2017). Neutrophil extracellular traps in immunity and disease. *Nature Reviews Immunology*, 18(2), 134–147. <https://doi.org/10.1038/nri.2017.105>
- Popovich, P. G., Guan, Z., McGaughy, V., Fisher, L., Hickey, W. F., & Basso, D. M. (2002). The neuropathological and behavioral consequences of intraspinal microglial/macrophage activation. *Journal of Neuropathology and Experimental Neurology*, 61(7), 623–633. <https://doi.org/10.1093/jnen/61.7.623>
- Popovich, P. G., & Jones, T. B. (2003). Manipulating neuroinflammatory reactions in the injured spinal cord: Back to basics. *Trends in Pharmacological Sciences*, 24(1), 13–17. [https://doi.org/10.1016/s0165-6147\(02\)00006-8](https://doi.org/10.1016/s0165-6147(02)00006-8)
- Prinz, M., Jung, S., & Priller, J. (2019). Microglia biology: One century of evolving concepts. *Cell*, 179(2), 292–311. <https://doi.org/10.1016/j.cell.2019.08.053>
- Rabchevsky, A. G., & Streit, W. J. (1998). Role of microglia in postinjury repair and regeneration of the CNS. *Mental Retardation and Developmental Disabilities Research Reviews*, 4(3), 187–192. [https://doi.org/10.1002/\(SICI\)1098-2779\(1998\)4:3<187::AID-MRDD6>3.0.CO;2-L](https://doi.org/10.1002/(SICI)1098-2779(1998)4:3<187::AID-MRDD6>3.0.CO;2-L)
- Sasaki, Y., Ohsawa, K., Kanazawa, H., Kohsaka, S., & Imai, Y. (2001). Iba1 is an actin-cross-linking protein in macrophages/microglia. *Biochemical and Biophysical Research Communications*, 286(2), 292–297. <https://doi.org/10.1006/bbrc.2001.5388>
- Subramanyam, C. S., Wang, C., Hu, Q., & Dheen, S. T. (2019). Microglia-mediated neuroinflammation in neurodegenerative

- diseases. *Seminars in Cell & Developmental Biology*, 94, 112–120. <https://doi.org/10.1016/j.semcdb.2019.05.004>
- Vaibhav, K., Braun, M., Alverson, K., Khodadadi, H., Kutiyawalla, A., Ward, A., Banerjee, C., Sparks, T., Malik, A., Rashid, M. H., Khan, M. B., Waters, M. F., Hess, D. C., Arbab, A. S., Vender, J. R., Hoda, N., Baban, B., & Dhandapani, K. M. (2020). Neutrophil extracellular traps exacerbate neurological deficits after traumatic brain injury. *Science Advances*, 6(22), eaax8847. <https://doi.org/10.1126/sciadv.aax8847>
- Wang, C., Wang, Y., Shi, X., Tang, X., Cheng, W., Wang, X., An, Y., Li, S., Xu, H., Li, Y., Luan, W., Wang, X., Chen, Z., Liu, M., & Yu, L. (2019). The TRAPs from microglial vesicles protect against listeria infection in the CNS. *Frontiers in Cellular Neuroscience*, 13(199), 199. <https://doi.org/10.3389/fncel.2019.00199>
- Webster, S. J., Daigneault, M., Bewley, M. A., Preston, J. A., Marriott, H. M., Walmsley, S. R., Read, R. C., Whyte, M. K. B., & Dockrell, D. H. (2010). Distinct cell death programs in monocytes regulate innate responses following challenge with common causes of invasive bacterial disease. *The Journal of Immunology*, 185(5), 2968–2979. <https://doi.org/10.4049/jimmunol.1000805>
- Weng, W., Hu, Z., & Pan, Y. (2022). Macrophage extracellular traps: Current opinions and the state of research regarding various diseases. *Journal of Immunology Research*, 2022, 7050807–10. <https://doi.org/10.1155/2022/7050807>
- Yona, S., Kim, K.-W., Wolf, Y., Mildner, A., Varol, D., Breker, M., Strauss-Ayali, D., Viukov, S., Guilliams, M., Misharin, A., Hume, D. A., Perlman, H., Malissen, B., Zelzer, E., & Jung, S. (2013). Fate mapping reveals origins and dynamics of monocytes and tissue macrophages under homeostasis. *Immunity*, 38(1), 79–91. <https://doi.org/10.1016/j.immuni.2012.12.001>
- Zivkovic, S., Ayazi, M., Hammel, G., & Ren, Y. (2021). For better or for worse: A look into neutrophils in traumatic spinal cord injury. *Frontiers in Cellular Neuroscience*, 15, 648076. <https://doi.org/10.3389/fncel.2021.648076>

## SUPPORTING INFORMATION

Additional supporting information can be found online in the Supporting Information section at the end of this article.

**How to cite this article:** Michel-Flutot, P., Bourcier, C. H., Emam, L., Gasser, A., Glatigny, S., Vinit, S., & Mansart, A. (2023). Extracellular traps formation following cervical spinal cord injury. *European Journal of Neuroscience*, 57(4), 692–704. <https://doi.org/10.1111/ejn.15902>